Proc. Inst. Electrostat. Jpn.

静電気学会誌, 19, 6 (1995) 444-451

論　　文

A Surface Charge Induction Electrostatic Motor

Jae-Duk MOON* and Dong-Hoon LEE**

(Received April 4, 1994)

A miniature size electrostatic induction motor has been fabricated and studied with emphasis on the role of the surface resistivity, the relative dielectric constant of the rotor surface materials and the rotor liner materials, which control the charge induction and relaxation on the rotor surface and the field intensity between the rotor and the stator. It is found that the surface resistivity and/or the relative dielectric constant of the rotor surface material influenced significantly the motor speed controlled by the surface charge induction and relaxation on the rotor surface depending on the applied voltage and/or frequency. The resistivity of the rotor liner material is also found to effect the motor speed greatly by control of the field intensity between the rotor and the stator and the surface charge distribution of the induced charge on the rotor. As a result, a maximum no load rotor speed of the motor tested was about 5500 rpm at the applied voltage of 4.5 kV and the frequency of 220 Hz for the case of the rotor surface material of $BaTiO_3$ 80% in the resin binder layered on the copper plate rotor liner material.

1. Introduction

Motors using an electrostatic force have a long history, Andrew Gordon built electrostatic motors in the 1850s, 100 years before the advent of magnetic electric motors.[1-3] Despite their distinguished history, electrostatic motors have found few practical applications because of the high voltage and the mechanical accuracy required. Recently electrostatic motors have been studied and developed by a number of researchers, because they have many advantages such as easier miniaturizing of the size to micrometer, higher torque compared with the size, gentler operation, and better mass production.[4-9]

Previous studies had been mostly focused on fabrication of a surface charge induction electrostatic motor with a constant rotor surface material.[4,5] And there are no papers to be studied on experimentally changing the properties of the surface and/or liner materials of the rotor, but theoretical expectations has been discussed only.[5] However in this paper it is tried to change the surface resistivity and the dielectric constant of the surface and liner material of the rotor. Because the most influencing parameter of this type of motor had been encountered as the surface charge induction and deduction on the rotor of the motor.[10-15] And, a miniature surface charge induction electrostatic motor has been designed and fabricated for the check of the parameters dominantly effecting characteristics of the motor, such as voltage and frequency of the 3 phase ac power supply, the surface resistivity and the relative dielectric constant of the rotor surface and liner materials.

Keywords : electrostatic motor, liner and surface, resistivity, dielectric constant, relaxation time constant

* Department of Electrical Engineering, College of Engineering, Kyungpook National University, 1370 Sankyuk-Dong, Buk-Ku, Taegu, Korea 702-701

** Department of Industrial Safety Engineering, College of Engineering, Pusan National University of Technology, 100 Yongdang-Dong, Nam-Ku, Pusan, Korea, 608-739

2. Experimental Methods and Apparatuses

2.1 An Electrostatic Induction Motor System Fabrication

Figure 1 shows a schematic diagram and a photograph of the electrostatic induction motor studied. The rotor was made of a top-and-bottom-closed hollow nylon-66 cylinder, having outer and inner diameters of 25.0 mm and 23.0 mm respectively, a length of 50.0 mm and a weight of 10.0 grams. The upper and lower side of the shaft of the rotor was supported by a bear-

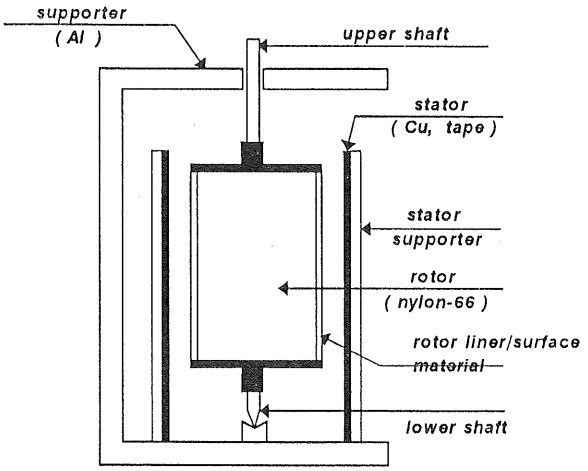

(a) Side view.

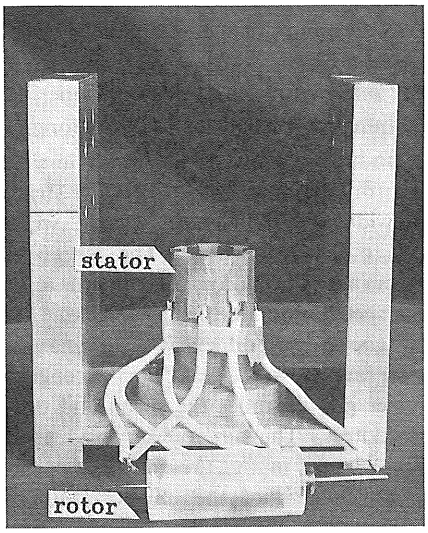

(c) Photograph.

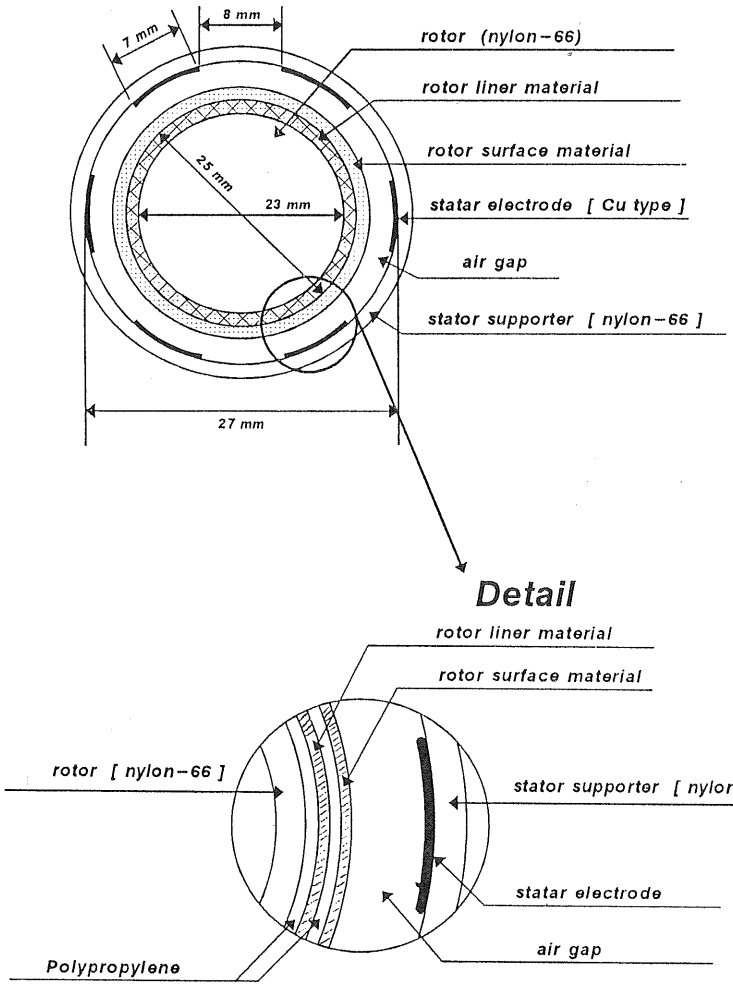

(b) Top view and closed up.

Fig. 1 Schematic diagram and photograph of electrostatic induction motor fabricated.

ing and a 2 mm diameter stainless steel pivot, respectively. The stator was also a hollow cylinder made of nylon-66 with an inner diameter of 27.0 mm and a length of 80.0 mm long.

On the inner surface of the stator, 6-electrodes, in the form of thin rectangular copper strips about 7 mm wide and interspaced 8 mm, were taped parallel to the rotor axis. The airgap between the rotor and the stator was determined to get higher speed and stronger torque. But, the shorter gap causes difficulty of mechanical construction and lower breakdown strength, while the longer gap degrades the speed and the torque of the motor. The airgap was fixed as approximately 0.5 mm in the present experiment. The design parameters of the electrostatic induction motor are listed in Table 1. The rotor speed was measured by a digital tacho-meter (Ono Sokki Co., Japan, HT431).

Figure 2 depicts the block diagram of the experimental power source, which consisted of a function generator, D/A converters, amplifiers and a high voltage transformer. The power was a controllable 3 phase ac having a voltage of 0–10 kV and a frequency range of 1～1,000 Hz. The waveform and magnitude of voltage were measured by an oscilloscope (Gold Star Co., Korea, 8020R) and digital voltmeters (Heung Chang Co., Korea, 601) and by high voltage probes (Keithley Co., England, 1600A).

2.2 The Surface and Liner Materials of the Rotor

It is known that an induction type electrostatic motor is influenced greatly by the properties of the material used, such as the resistivity and the dielectric constant of the rotor surface and the liner material,[5] which control the charge induction and distribution, and the electric field intensity in the airgap. A polypropylene sheet (PP, 90±5 μm thick) was used as a base material for the rotor surface and liner. The electrical properties of the surface and liner material of the rotor were changed. Two methods were introduced to change the properties. An electron beam depositor (Anelva Co., Japan, EVD500A) was used to deposit Ni (10～20 Å thick, Katayama Chemical Co., Japan, 4N) and Ti (5～50 Å thick, Rare Metal Co., Japan, 4N) on the PP to control the surface resistivity, ϱ_s. Screen print method was used to coat TiO_2 (20 μm±2 μm thick) or $BaTiO_3$ (20 μm±2 μm thick) powder (Aldrich Co., USA) on the PP to control the relative dielectric constant, ε_r.

All experiments were carried out in an electromagnetically shielded room. Each parameters, ϱ_s and ε_r, were measured with a resistivity meter (Hewlett Packard Co., USA, 4329A) and a digital LCR meter (ED Engineering Co., Korea, EDC-1620) in the electromagnetically shielded room at 20°C and 35% RH. The relaxation time constant, $\tau=\varepsilon_0\varepsilon_r\varrho_s$, was calculated from the measured ε_r and ϱ_s at the present experiments, and ε_0 is the dielectric constant in vacuum. Tables 2 and 3 indicate the electrical properties for the rotor materials used.

3. Experimental Results and Considerations

Figure 3 shows the motor speed as a function of the applied frequency of the 3 phase ac voltage

Table 1 Specifications of fabricated motor.

Specifications of motor tested	
Airgap, g	0.5 mm
Outer diameter of rotor, d_{or}	25.0 mm
Inner diameter of rotor, d_{ir}	23.0 mm
Length of rotor, l_r	50.0 mm
Weight of rotor, m	10.0 g
Surface area of rotor, s	98.2×10^3 mm^2
Diameter of stator, d_s	27.0 mm
Width of stator electrode, w	7.0 mm
Interelectrode spacing of stator electrode, t	8.0 mm
Number of pole, p	3
Pole pitch, p_p	2
Applied voltage to the motor tested, V	0–5100 V
Applied frequency to the motor tested, f	0–300 Hz

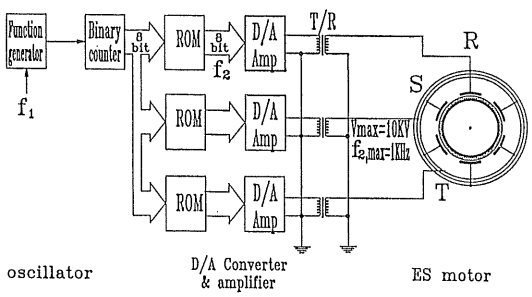

Fig. 2 Block diagram of 3 phase variable frequency and voltage power source.

Table 2 Electric characteristics of rotor materials.

Surface materials of the rotor	Surface resistivity $\varrho_s(\Omega/\square)$	Symbol
Polypropylene	8.5×10^{11}	PP
PP on which Ti 5 Å was deposited	4.3×10^{11}	Ti 5 Å
PP on which Ti 10 Å was deposited	3.2×10^{11}	Ti 10 Å
PP on which Ti 20 Å was deposited	2.8×10^{11}	Ti 20 Å
PP on which Ti 30 Å was deposited	3.4×10^{10}	Ti 30 Å
Copper tape	0	Cu
PP on which Ti 40 Å was deposited	3.4×10^{9}	Ti 40 Å
PP on which Ti 50 Å was deposited	2.6×10^{9}	Ti 50 Å
PP on which Ni 10 Å was deposited	1.4×10^{8}	Ni 10 Å
PP on which Ni 15 Å was deposited	2×10^{6}	Ni 15 Å
PP on which Ni 20 Å was deposited	2×10^{5}	Ni 20 Å

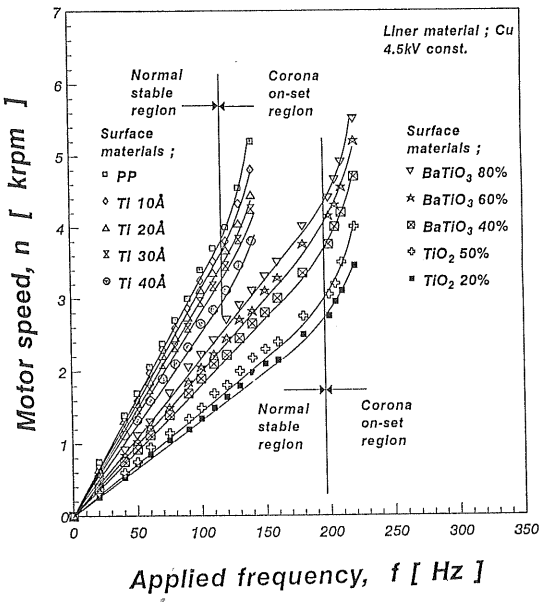

Fig. 3 Motor speed as a function of power frequency for different surface material at constant applied voltage.

Table 3 Electric characteristics of rotor materials.

Surface material of the rotor	Dielectric constant (ε_r) at 120 Hz	Surface resistivity ϱ_s ($\Omega/\square$)	Relaxation time constant $\tau=\varepsilon_0\varepsilon_r\varrho_s$	Symbol
Polypropylene	2.2	8.5×10^{11}	16.56	PP
PP+Binder+10% TiO_2	10.5	0.6×10^{10}	0.56	TiO_2 10%
PP+Binder+20% TiO_2	12.5	0.6×10^{10}	0.64	TiO_2 20%
PP+Binder+30% TiO_2	14.3	0.6×10^{10}	0.76	TiO_2 30%
PP+Binder+50% TiO_2	20.7	0.7×10^{10}	1.28	TiO_2 50%
PP+Binder+70% TiO_2	38.6	0.8×10^{10}	2.73	TiO_2 70%
PP+Binder+10% $BaTiO_3$	19.2	0.7×10^{10}	1.19	$BaTiO_3$ 10%
PP+Binder+20% $BaTiO_3$	27.6	0.8×10^{10}	1.96	$BaTiO_3$ 20%
PP+Binder+30% $BaTiO_3$	33.7	0.8×10^{10}	2.39	$BaTiO_3$ 30%
PP+Binder+40% $BaTiO_3$	45.9	0.8×10^{10}	3.25	$BaTiO_3$ 40%
PP+Binder+50% $BaTiO_3$	57.3	0.8×10^{10}	4.06	$BaTiO_3$ 50%
PP+Binder+60% $BaTiO_3$	63.9	0.9×10^{10}	5.09	$BaTiO_3$ 60%
PP+Binder+70% $BaTiO_3$	75.5	0.8×10^{10}	5.35	$BaTiO_3$ 70%
PP+Binder+80% $BaTiO_3$	85.4	1.1×10^{10}	8.32	$BaTiO_3$ 80%

for 10 different rotor surface materials at a constant applied voltage of 4.5 kV, where the rotor liner material was fixed to the copper plate. The motor speed was increased linearly with increase of the applied frequency. But the speed increased nonlinearly at high frequency (120 Hz for the Ti deposited, 200 Hz for the $BaTiO_3$ and TiO_2 coated), at which coronas were observed in the airgap. However, it is found that the speed of the motor could be controlled linearly by changing the applied frequency. Figure 3 shows the effects of ϱ_s and ε_r of the rotor materials. When Ti was deposited on the PP, the heavier deposited ones showed the lower speed at the constant

applied voltage and frequency, while the heavier coated $BaTiO_3$ and TiO_2 showed the higher speed. It is found that ϱ_s and ε_r influenced greatly to the speed of the induction type electrostatic motor.

Figure 4 shows the induced partial discharge onset voltage between the rotor and the stator as a function of applied frequency at the rotor liner material of copper plate. The induced partial discharge onset voltages of both Ti and Ni deposited and $BaTiO_3$ and TiO_2 coated decrease linearly with increase of the applied frequency. Hence the frequency of the ac power source is thought to be the most predominant parameter to this capacitive load of the motor. As shown in Figure 4, this type of the motor should be operated within the frequency at where the partial discharge between the rotor and the stator does not occur.

Figures 5 and 6 show the motor speed as a function of applied voltage at the frequency of 40, 50, 90, 120, and 160 Hz, respectively, for different surface materials and fixed liner material of copper plate. In Figure 5 there are 3 different stages on the motor operation; that is, first stage: motor stop stage at the lower applied voltage, second stage: normal stable stage, and third stage: abnormal speed stage at the higher applied voltage. The motor did not move at voltages below 3.3 kV for the case of Figure 5, and 4.0 kV for the case of Figure 6, because of small torque. While at the higher voltages partial discharges were occurred in the airgap between the rotor and the stator. It is not clear that the partial discharge makes the speed of the motor abnormally increase, which, however, would be studied in

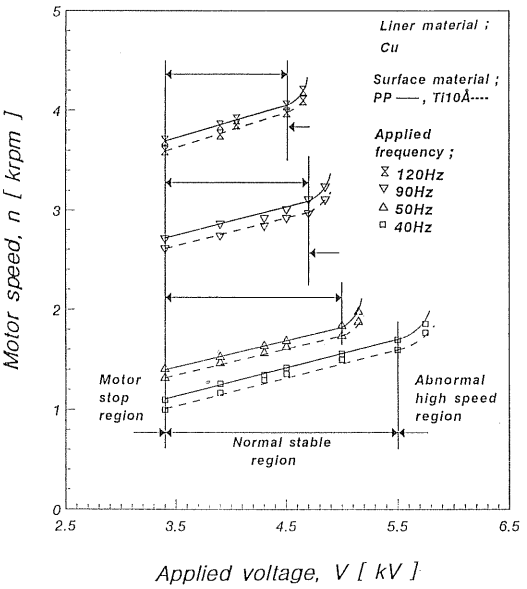

Fig. 5 Motor speed as a function of applied voltage at the Ti 10 Å deposited rotor surface and at the different power frequency.

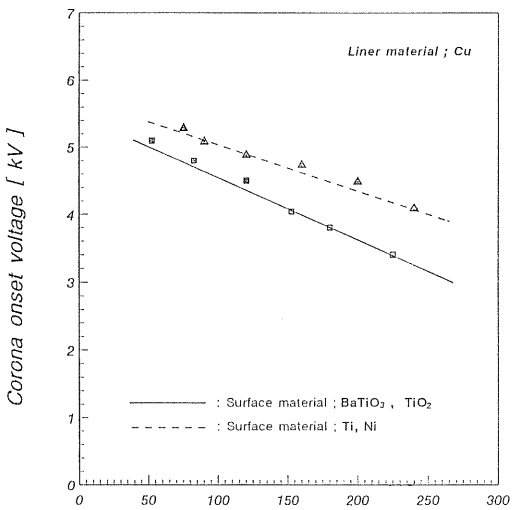

Fig. 4 Corona onset voltage as a function of power frequency for different surface material.

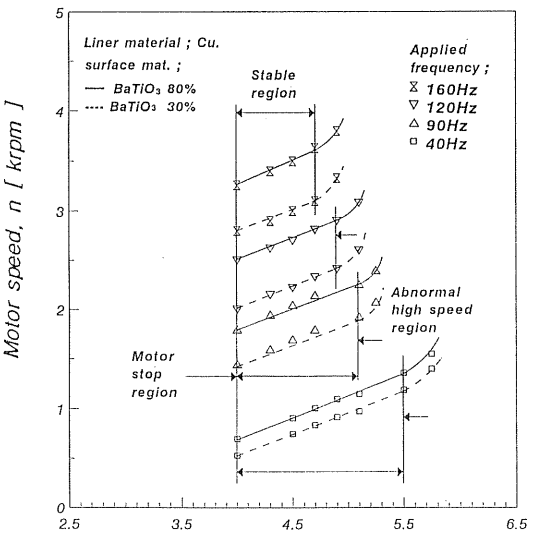

Fig. 6 Motor speed as a function of applied voltage at the $BaTiO_3$ coated rotor surface and at the different power frequency.

detail in the near future. In the normal stable stage, the motor speed to the unit applied voltage was 150 rpm/kV. As a result the motor should qe operated at second stage, the normal stable stage.

The speed characteristics of the $BaTiO_3$ deposited ones were almost the same as those of Ti deposited ones, as shown in Figure 6. It showed the motor speed to the unit applied voltage of 480 rpm/kV, which was about 3 times higher than that of the Ti deposited one shown in Figure 5.

As is shown in Figure 3, the speed characteristics of the surface charge induction electrostatic motor were influenced dominantly by the phase changing of the applied power source, the electrical properties of the rotor surface and liner matetials. Which means that the surface resistivity and the relative dielectric constant of the rotor surface material would control induction and relaxation of the appearent charge onto the surface of the rotor, while the rotor liner material adjusts the electric field intensity uniformly onto the rotor surface.[5,14,15]

Figure 7 shows the motor speed as a function of surface resistivity of the different rotor liner material at a constant applied voltage of 4.5 kV and a constant frequency of 60 Hz. The motor speed increased linearly with decrease of the surface resistivity of the rotor liner material. It was shown that the induced and dipolarized charges just on the surface of the material of the rotor were arranged uniformly by decreasing the surface resistivity of the rotor liner material, which also might increase the maximum mean quantity of the induced charge on the rotor surface without any partial discharge occurrence.

Figure 8 shows the motor speed as a function of surface resistivity of the rotor surface material for different liner material at a constant voltage of 4.5 kV and a constant frequency of 60 Hz. The motor speed increased slowly with increase of the surface resistivity of the rotor surface materials, and saturated at above 10^{12} $\Omega/\square$ of the surface resistivity. It shows that the higher resistivity of the liner material gives the higher speed of the motor.

Figure 9 shows the motor speed as a function of relative dielectric constant, ε_r, of the rotor surface materials at different voltages of 4.1 kV, 4.5 kV, 4.75 kV, 4.9 kV and 5.1 kV, and at a constant frequency of 60 Hz. At voltages of 4.1 kV, 4.5 kV and 4.75 kV, the motor speed slowly increased with increase of ε_r up to $\varepsilon_r = 50$, but above this value, $\varepsilon_r \geq 60$, the motor speed was saturated. While at the higher voltage of 4.9 kV, the motor speed rapidly increased with increase of ε_r until $\varepsilon_r = 50$, but at above $\varepsilon_r = 60$ the motor

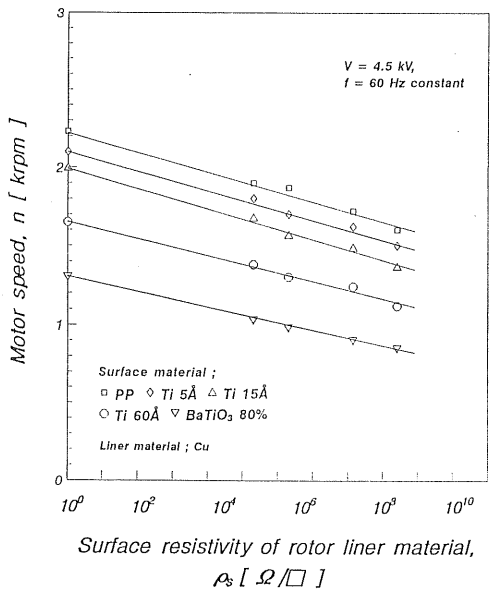

Fig. 7 Motor speed as a function of surface resistivity of rotor liner material for different rotor surface material.

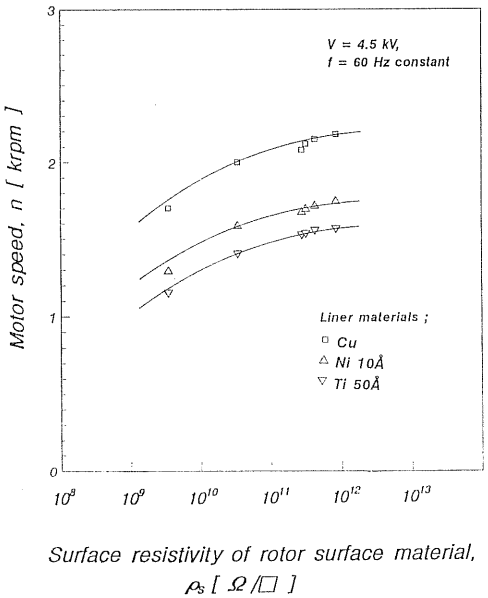

Fig. 8 Motor speed as a function of surface resistivity of rotor surface material at different liner material.

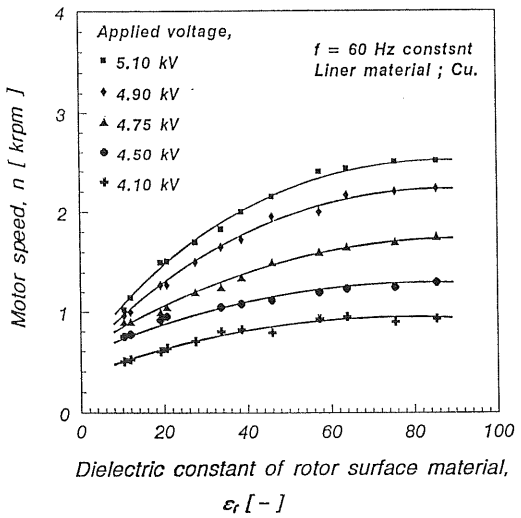

Fig. 9 Motor speed as a function of dielectric constant of rotor surface material at different applied voltage.

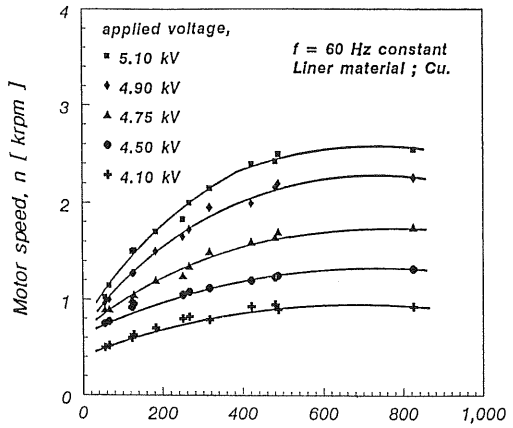

Fig. 10 Motor speed as a function of relaxation time constant of rotor surface material at different applied voltage.

speed was also saturated. The reason for increase of the motor speed would be due to the increased charge density of the rotor surface by proportionally increasing the relative dielectric constant of the rotor surface material.

Figure 10 shows comparisons of the motor speed as a function of relaxation time constant, $\tau=\varepsilon_0\varepsilon_r\varrho_s$, of the rotor surface material. Since τ in Figure 10 was calculated from the measured values of the particular cases of the present experiment, and the dimensions of τ are indicated in Figure 10. It is shown that the motor speed was influenced strongly by the charge relaxation time constant of the motor surface material. The motor speed increased with increase of the relative relaxation time constant of the induced charge, but at the higher value of $\tau\geq 5$, the motor speed was saturated.

As shown in Figures 7, 8, 9 and 10, the higher resistivity and/or relative dielectric constant, concurrently the long relative relaxation time constant, cause the higher motor speed, while the lower resistivity of the rotor liner materials gives the higher speed at the present experiment cases.

4. Conclusions

A miniature size surface charge induction electrostatic motor has been fabricated and studied on the parameters influencing dominantly the motor speed, such as voltage and frequency of the 3 phase ac power supply, the surface resistivity, the relative dielectric constant, and the calculated relative relaxation time constant of the rotor surface materials, and the surface resistivity of the rotor liner materials. The following conclusions are derived:

(1) The no load motor speed was proportional to the applied 3 phase ac voltage. There are 3 different stages on the electrostatic motor operation, that is, motor stop region, normal and stable region, and abnormal speed region. As a result, the model motor should be operated at the normal stable region.

(2) The motor speed was increased linearly with increase of the applied voltage and frequency of the 3 phase ac power supply, but it had critical value at the higher frequency where the partial discharges take place in the airgap between the rotor and the stator. This characteristic makes it possible to control the motor speed linearly by changing the applied voltage and frequency which could be used very conveniently for practical operation.

(3) From the parametric studies, the higher resistivity and/or relative dielectric constant, and concurrently the longer relative relaxation time constant of the rotor surface materials give the higher speed. While the lower resistivity of the rotor liner material gives the higher speed.

References

1) P. Benjamin: *A History of Electricity*, p. 506, John Wiley & Sons, USA (1898)
2) The Institute of Electrostatics Japan: *Electrostatic Handbook*, p. 664, Ohm, Japan (1986)
3) O. D. Jefimenko: *Electrostatic Motors*, Electret Science Company, Star City, USA (1973)
4) S. D. Choi and D. A. Dunn: Proc. of IEEE, **59** (1971) 737
5) E. R. Mognaschi and J. H. Calderwood: IEE Proceedings, **137**, Pt. A, No. 6 (1990) 331
6) M. Hattory and K. Asano: *Proc. of the Institute of Electrostatics Japan*, p. 81 (1991)
7) L.-S. Fan, Y.-C. Tai and R. S. Muller: Sensors and Actuators, **20** (1989) 41
8) W. S. N. Trimmer and K. J. Gabriel: Sensors and Actuators, **11** (1987) 189
9) S. F. Bart and J. H. Lang: Sensors and Actuators, **20** (1989) 97
10) J.-D. Moon and D.-H. Lee: The Journal of The Korean Institute of Electrical Engineers, **40** (1991) 7
11) J.-D. Moon and D.-H. Lee: *Proc. of The Conference of The Korean Institute of Electrical Engineers*, p. 322 (1991)
12) J.-D. Moon and D.-H. Lee: *Proc. of The Conference of The Korean Institute of Electrical Engineers*, p. 522 (1992)
13) J.-D. Moon and D.-H. Lee: *Proc. of The Third Conference on Sensor Technology of The Korean Sensors Society*, p. 110 (1992)
14) D.-H. Lee: *Proc. of The Institute of Electrostatics Japan, International Session*, p. 77 (1992)
15) J.-D. Moon and D.-H. Lee: Journal of The Korean Sensors Society, **2** (1993) 65